

# Segmental Relaxation Characteristics of Cross-Linked Poly(ethylene oxide) Copolymer Networks

Sumod Kalakkunnath,<sup>†</sup> Douglass S. Kalika,<sup>\*,†</sup> Haiqing Lin,<sup>‡</sup> and Benny D. Freeman<sup>‡</sup>

Department of Chemical and Materials Engineering and Center for Manufacturing, University of Kentucky, Lexington, Kentucky 40506-0046, and Center for Energy and Environmental Resources, Department of Chemical Engineering, University of Texas at Austin, Austin, Texas 78758

Received August 4, 2005; Revised Manuscript Received September 3, 2005

**ABSTRACT:** The segmental relaxation characteristics of UV cross-linked networks based on poly(ethylene glycol) diacrylate [PEGDA] copolymerized with either poly(ethylene glycol) methyl ether acrylate [PEGMEA] or poly(ethylene glycol) acrylate [PEGA] were investigated using dynamic mechanical analysis. The molecular weights of the PEGDA cross-linker and acrylate comonomers were selected to obtain rubbery, amorphous membrane materials with constant ethylene oxide content. The introduction of PEGMEA or PEGA in the reaction mixture was used to control cross-link density and led to the insertion of flexible oligomeric branches within the resulting networks. For both copolymer series, the introduction of acrylate comonomer led to a decrease in glass transition temperature ( $T_g$ ) and a systematic reduction in cross-link density; the downward shift in  $T_g$  was much more pronounced for the PEGDA/PEGMEA copolymers. Time–temperature superposition was used to construct modulus master curves across the glass transition, and these could be satisfactorily fit using the Kohlrausch–Williams–Watts (KWW) function. The KWW curve fits indicated a narrowing of the glass–rubber relaxation with reduced cross-link density that correlated with a decrease in fragility for the networks. Gas transport measurements revealed a strong sensitivity to copolymer composition for the PEGDA/PEGMEA networks (–OCH<sub>3</sub> branch end group) as compared to the PEGDA/PEGA networks (–OH end group), with CO<sub>2</sub> permeability and CO<sub>2</sub>/H<sub>2</sub> selectivity increasing with increased branch content in the PEGDA/PEGMEA membranes. Both the observed glass transition and transport behavior correlated with measured variations in fractional free volume for these networks.

## Introduction

The selective removal of carbon dioxide from mixtures containing light gases is a process of immense industrial importance, and there is growing interest in the implementation of membrane technologies to achieve such separations for a number of applications, e.g., the separation of CO<sub>2</sub> from hydrogen upon steam reforming of hydrocarbons or the removal of CO<sub>2</sub> from CH<sub>4</sub> for natural gas purification.<sup>1</sup> For many of these applications, membrane materials with high CO<sub>2</sub> permeability and high CO<sub>2</sub>/light gas selectivity are desired, so that the CO<sub>2</sub> will permeate to the low-pressure side of the membrane, while the light gas component is retained at or near the feed pressure for subsequent transport and use. One method to achieve membranes with high CO<sub>2</sub> permeability and favorable overall CO<sub>2</sub> selectivity is to select and/or tailor materials with high CO<sub>2</sub> solubility and high CO<sub>2</sub>/light gas solubility selectivity. The quadrupolar character of CO<sub>2</sub> can be exploited in this regard, since CO<sub>2</sub> will tend to interact favorably with polar groups present in the membrane.<sup>2</sup> A recent review of potential CO<sub>2</sub> interactions has shown ether oxygens to be among the most promising polar groups for the achievement of favorable CO<sub>2</sub> solubility and solubility selectivity.<sup>3</sup> The formulation of rubbery polymeric materials incorporating high levels of the flexible ether oxygen moieties should lead to membranes with strong CO<sub>2</sub> solubility as well as high diffusivity. The net result would be membranes with the potential to deliver

the desired separation properties in terms of overall CO<sub>2</sub> permeability as well as the purity of the resulting product streams.

Poly(ethylene oxide) [PEO;  $-(\text{--OCH}_2\text{CH}_2\text{--})_n\text{--}$ ] has been identified as an effective membrane material for the selective separation of quadrupolar–nonpolar gas pairs.<sup>4</sup> However, PEO has a strong tendency to crystallize, and the presence of a significant crystalline fraction reduces permeability in these materials to nonviable levels for industrial separations. One approach to inhibit crystallization in PEO is the introduction of chemical cross-links. By limiting the number of ethylene oxide segments ( $n$ ) between cross-link junctions to about 20 or less, fully amorphous cross-linked networks can be obtained.<sup>5,6</sup> The possibility of preparing wholly amorphous networks with high ethylene oxide content suggests a number of potential membrane architectures that could be designed to achieve optimum CO<sub>2</sub> permeability and selectivity characteristics.

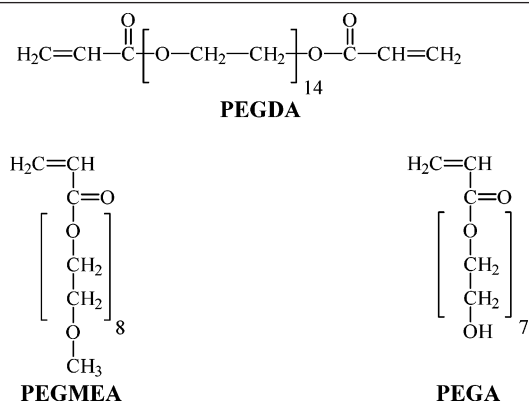
The successful preparation of PEO-based membranes with high CO<sub>2</sub> permeability as well as high CO<sub>2</sub>/light gas selectivity requires fundamental insight as to the relationships between the gas transport properties and the structural and dynamic characteristics of the materials. In this paper, two series of PEO networks based on the ultraviolet (UV) photopolymerization of poly(ethylene glycol) diacrylate [PEGDA] have been investigated using dynamic mechanical analysis. The focus is on assessing how systematic variations in cross-link density affect the physical and gas transport characteristics of the membranes. To vary cross-link density, PEGDA is copolymerized with either poly(ethylene glycol) methyl ether acrylate [PEGMEA] or poly-

<sup>†</sup> University of Kentucky.

<sup>‡</sup> University of Texas at Austin.

\* Corresponding author: Tel 859-257-5507; Fax 859-323-1929; e-mail kalika@engr.uky.edu.

**Table 1. Chemical Structures of Poly(ethylene glycol) Diacrylate [PEGDA], Poly(ethylene glycol) Methyl Ether Acrylate [PEGMEA], and Poly(ethylene glycol) Acrylate [PEGA] with Monomeric Repeat Values ( $n$ ) as Indicated**



(ethylene glycol) acrylate [PEGA] (see chemical structures in Table 1). The inclusion of monofunctional acrylate in the reaction mixture leads to the introduction of fixed-length pendant groups in the resulting cross-linked network as well as an increase in the distance between cross-links, as illustrated in Figure 1. For this study, the molecular weights of the acrylates (PEGMEA and PEGA) were selected so as to maintain an approximately constant ethylene oxide (EO) content in the networks ( $\sim 82$  wt % EO). As a result, any measured changes in gas transport properties can be attributed to structural variations, i.e., changes in the cross-link density as well as the nature of the pendant chain end.

A number of studies have been undertaken to assess the influence of cross-linking on the segmental relaxation properties of polymer networks; both dynamic mechanical analysis and broadband dielectric spectroscopy have been successfully applied to elucidate the influence of cross-link density on the glass transition temperature as well as on the time–temperature characteristics of the glass–rubber relaxation.<sup>7–16</sup> In general, the introduction of chemical cross-links results in a restriction of segmental mobility in the vicinity of the cross-link junctions, and this constraint is manifested to varying extents depending upon the physical property under consideration. For example, the glass transition temperature,  $T_g$ , is observed to increase with increasing cross-link density, with the most pronounced offset evident at high cross-link densities where the average distance between cross-links approaches the characteristic length scale for segmental motion.<sup>8</sup> In addition, the presence of the cross-links leads to an inhomogeneous broadening of the glass–rubber relaxation that reflects the range of motional environments experienced by the relaxing segments and their relative proximity to the cross-link junctions. For the copolymer systems investigated here, cross-link density will be varied by the inclusion of different amounts of acrylate (i.e., PEGMEA, PEGA) in the reaction mixture. As a result, the measured dynamic relaxation characteristics will be influenced not only by changes in cross-link density but also by the presence of nonreactive oligomeric pendant groups in the network.<sup>15</sup> The maximum effective cross-link density in these materials is determined by the molecular weight of the PEGDA cross-linker, which has a corresponding monomeric repeat length  $n = 14$  (14 ethylene oxide units).

In this study, dynamic mechanical measurements were performed for two series of copolymer networks based on PEGDA ( $n = 14$ ): PEGDA-*co*-PEGMEA and PEGDA-*co*-PEGA. The reactants were selected so as to maintain an approximately constant ethylene oxide content for all network compositions. The key difference between the two copolymer series is the end group associated with the acrylate species:  $-\text{OCH}_3$  (PEGMEA) vs  $-\text{OH}$  (PEGA). By application of time–temperature superposition methods,<sup>17</sup> it was possible to establish modulus–frequency master curves over the entire range of the glass–rubber relaxation, and the resulting curves could be satisfactorily fit using the Kohlrausch–Williams–Watts (KWW) stretched exponential function.<sup>18</sup>  $T_g$ -normalized Arrhenius plots (i.e., fragility or cooperativity plots<sup>7,19</sup>) were used to assess changes in intermolecular cooperativity across the glass transition with varying network structure. The characteristics of the copolymer networks were subsequently related to their gas transport properties.

## Experimental Section

**Materials.** Poly(ethylene glycol) diacrylate (PEGDA: MW = 700 g/mol), poly(ethylene glycol) methyl ether acrylate (PEGMEA: MW = 460 g/mol), and poly(ethylene glycol) acrylate (PEGA: MW = 380 g/mol) were purchased from Aldrich Chemical Co. (Milwaukee, WI); the nominal molecular weights provided by the supplier are as given above. 1-Hydroxycyclohexyl phenyl ketone [HCPK] initiator was also purchased from Aldrich. All reagents were used as received.

Proton nuclear magnetic resonance ( $^1\text{H}$  NMR) and fast atom bombardment mass spectrometry (FAB-MS) were used to verify the molecular weight of the prepolymers. For PEGDA,  $^1\text{H}$  NMR indicated a value of 743 g/mol, which corresponds to a monomeric repeat value of  $n \sim 14$ . For the acrylates, the measured values were PEGMEA ( $n = 8.5$ ) and PEGA ( $n = 7$ ). In addition, FAB-MS measurements indicated a narrow distribution of molecular weight in all cases (polydispersity index  $< 1.10$ ). These measurements were in good agreement with the values reported by the supplier; additional experimental details are presented in a previous paper.<sup>20</sup>

**Polymer Preparation.** The prepolymer mixtures were prepared by adding 0.1 wt % initiator (HCPK) to an appropriate liquid blend of PEGDA with either PEGMEA or PEGA. After stirring, the mixture was sonicated for 10 min to eliminate bubbles (Ultrasonic cleaner, model FS60, Fisher Scientific, Pittsburgh, PA). The liquid was sandwiched between two quartz plates, which were separated by spacers to control film thickness. The mixture was polymerized by exposure to 312 nm UV light in a UV cross-linker (model FB-UVXL-1000, Fisher Scientific) for 90 s at 3 mW/cm<sup>2</sup>. The solid films obtained by this process were three-dimensional networks and contained a negligible amount of low molecular weight polymer (i.e., sol) that was not bound to the network. The as-synthesized films were immersed in a large amount of ultrapure water for at least 5 days to allow any residual sol to diffuse out of the films. The water was changed daily.

Attenuated total reflection Fourier transform infrared spectroscopy (FTIR-ATR) was used to determine the conversion of acrylate groups in the films (see ref 20). In all cases, essentially 100% conversion of the acrylate species was achieved.

**Dynamic Mechanical Analysis.** Dynamic mechanical thermal analysis was performed using a Polymer Laboratories DMTA operating in single cantilever bending geometry. The polymer films had a thickness of 1.0 mm and were dried under vacuum at room temperature prior to measurement. Storage modulus ( $E'$ ) and loss tangent ( $\tan \delta$ ) were recorded at a heating rate of 1 °C/min with test frequencies in the range of 0.1–10 Hz; all measurements were carried out under an inert ( $\text{N}_2$ ) atmosphere.

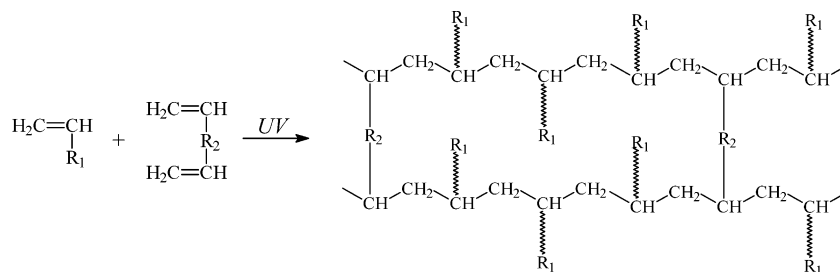


**Figure 1.** Schematic representation of ideal diacrylate/acrylate cross-linked copolymer network.

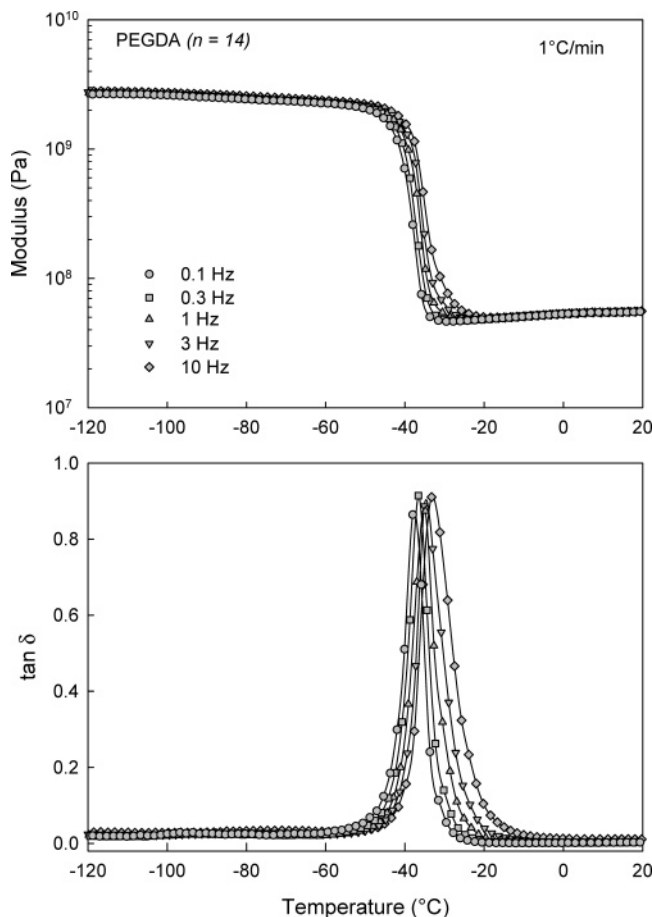


**Figure 2.** Dynamic mechanical properties ( $E'$ ;  $\tan \delta$ ) vs temperature for 100% PEGDA ( $n = 14$ ) network; heating rate of 1 °C/min.

## Results and Discussion

**Glass–Rubber ( $\alpha$ ) Relaxation.** Dynamic mechanical results over the entire temperature range studied (−120 to 20 °C) are presented for the 100% PEGDA network in Figure 2. Storage modulus and  $\tan \delta$  are plotted isochronally for five measurement frequencies ranging from 0.1 to 10 Hz. The data show a clear, stepwise decrease in modulus centered at −35 °C that corresponds to the glass–rubber relaxation in these fully cross-linked networks. The drop in modulus is accompanied by a narrow peak in  $\tan \delta$  which shifts to higher temperatures with increasing frequency (i.e., decreasing experimental time scale). The nominal glass transition temperature,  $T_\alpha$ , is defined here as corresponding to the peak in  $\tan \delta$  at a frequency of 1 Hz. For 100% PEGDA,  $T_\alpha = -35$  °C.

Results for the PEGDA/PEGMEA series of copolymers (1 Hz) are presented in Figure 3. For the various copolymer samples studied, the ratio of PEGDA to

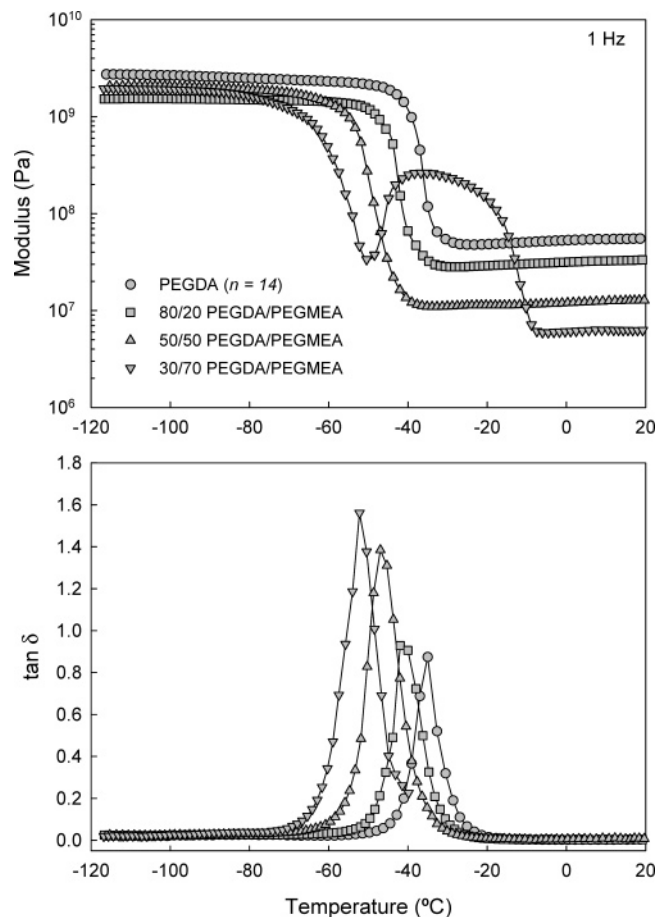


**Figure 3.** Dynamic mechanical properties ( $E'$ ;  $\tan \delta$ ) vs temperature for PEGDA/PEGMEA copolymer networks. Frequency of 1 Hz; heating rate of 1 °C/min.

PEGMEA in the initial reaction mixture is indicated on a weight basis (e.g., 80/20 PEGDA/PEGMEA corresponds to a network based on 80 wt % PEGDA, 20 wt % PEGMEA). The data show a progressive decrease in the glass–rubber relaxation temperature with PEGMEA content, as both the step change in  $E'$  and peak in  $\tan \delta$  are shifted to the left with increasing PEGMEA. The  $T_\alpha$  values for the series are reported in Table 2 as well as glass transition temperatures ( $T_g$ ) determined by DSC.<sup>21</sup> The  $T_\alpha$  and  $T_g$  values show good overall correspondence. The small, consistent difference between  $T_\alpha$  and  $T_g$  (~5 °C) reflects the inherent difference in experimental time scale for the dynamic mechanical (1 Hz) and DSC measurements.

The introduction of an increasing amount of PEGMEA in the reaction mixture leads to a corresponding decrease in the cross-link density of the network. This decrease in cross-link density is manifested by a decrease in the storage modulus in the rubbery plateau region ( $E_R$ ). For the 30/70 PEGDA/PEGMEA sample,



Table 2. Characteristics of Cross-Linked PEGDA and Copolymer Networks<sup>a</sup>

	$T_{\alpha}$ (1 Hz), °C	$T_g$ (DSC), °C	$T_{\beta}$ (10 Hz), °C	$\beta_{\text{KWW}}$	FFV
PEGDA	-35	-40	-70	0.30	0.118
PEGDA/PEGMEA					
80/20	-41	-44	-77	0.33	0.122
50/50	-47	-52	-79	0.34	0.127
30/70	-52	-57	-82		0.128
PEGDA/PEGA					
80/20	-38	-40	-73	0.34	0.112
50/50	-41	-42	-73	0.35	0.112
30/70	-42	-44		0.38	0.110

<sup>a</sup>  $T_{\alpha}$  is the dynamic mechanical peak temperature for glass transition (1 Hz),  $T_g$  the calorimetric glass transition temperature,<sup>21</sup>  $T_{\beta}$  the dynamic mechanical peak temperature for sub-glass transition (10 Hz),  $\beta_{\text{KWW}}$  the KWW distribution parameter for glass–rubber relaxation, and FFV the fractional free volume based on density measurements.<sup>21</sup>

the cross-link density is insufficient to fully suppress PEO crystallization in the network. This is evident in the modulus–temperature curve for the 30/70 specimen, which shows an increase in  $E'$  just above the glass transition that appears to correspond to the onset of cold crystallization. For the dynamic mechanical measurements, the samples were mounted in the DMTA at room temperature and then cooled rapidly to the start temperature of  $-120$  °C (effective cooling rate of  $-15$  °C/min). Given the relatively rapid cooling rate, it is likely that the sample initially contained little or no crystallinity. The subsequent dynamic mechanical heating scan was conducted at a much slower rate ( $+1$  °C/min), allowing the sample ample time to crystallize in-situ upon passing the glass transition, followed eventually by the onset of melting at  $-20$  °C. The room temperature modulus then corresponds to a fully amorphous, rubbery material. The observed behavior is consistent with DSC sweeps ( $20$  °C/min) conducted on these copolymers, which showed cold crystallization exotherms for copolymers containing high levels of PEGMEA.<sup>21</sup>

The decrease in glass transition temperature observed for the PEGDA/PEGMEA series is attributable primarily to the introduction of pendant groups along the network backbone. In a complementary study,<sup>20,22</sup> PEGDA ( $n = 14$ ) networks with varying cross-link density were prepared by the introduction of increasing amounts of water diluent in the prepolymer reaction mixture. The presence of the diluent led to the formation of “wasted” cross-links (e.g., loops) that did not contribute to the elastic character of the network, resulting in a decrease in the effective cross-link density as determined by dynamic mechanical as well as swelling measurements. For these PEGDA/water networks, no variation in  $T_{\alpha}$  or fractional free volume (FFV) was observed with varying effective cross-link density. By contrast, for the PEGDA/PEGMEA films, a significant decrease in  $T_{\alpha}$  is encountered with the reduction in cross-link density that accompanies copolymerization of the PEGMEA. A systematic increase in FFV for the PEGDA/PEGMEA films is also observed over the range of compositions examined (see Table 2).<sup>21</sup> Although the topographical details for the PEGDA/water and PEGDA/PEGMEA systems are likely to be quite different, the contrast in their glass transition characteristics suggests that the key structural element for the observed behavior in the PEGDA/PEGMEA series is the flexible pendant branches, which lead to both a greater fractional free volume and a correspondingly shorter relaxation time.

Dynamic mechanical data for the PEGDA/PEGA series are provided in Figure 4. The results are similar to those obtained for the PEGDA/PEGMEA specimens,

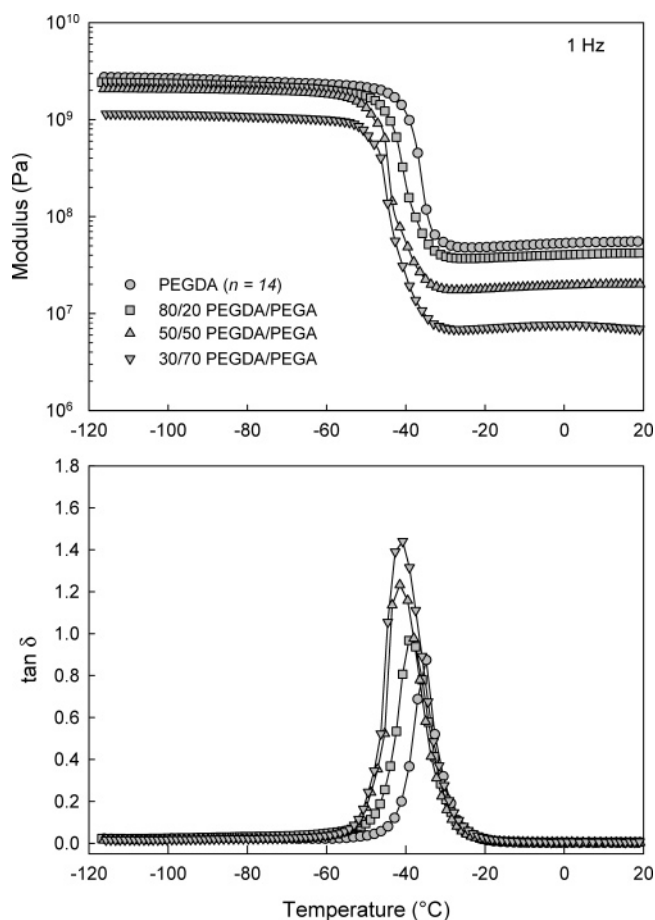


**Figure 4.** Dynamic mechanical properties ( $E'$ ;  $\tan \delta$ ) vs temperature for PEGDA/PEGA copolymer networks. Frequency of 1 Hz; heating rate of  $1$  °C/min.

with both a negative shift in  $T_{\alpha}$  and a progressive decrease in rubbery modulus observed with increasing PEGA content. For the PEGDA/PEGA series, however, the relative downward shift in relaxation temperature over the composition range is much less ( $\Delta T_{\alpha} = T_{\alpha}^{30/70} - T_{\alpha}^{100/0} = -7$  °C) as compared to the PEGDA/PEGMEA system ( $\Delta T_{\alpha} = -17$  °C). Also, neither crystallization nor melting is observed during the dynamic mechanical scans. As noted above, the main structural difference between the PEGMEA and PEGA components is the pendant end group, i.e.,  $-\text{OCH}_3$  vs  $-\text{OH}$ .

**Sub-Glass ( $\beta$ ) Relaxation.** Dynamic mechanical results in the sub-glass transition region are presented as plots of  $\tan \delta$  vs temperature (10 Hz) in Figure 5 (PEGDA/PEGMEA) and Figure 6 (PEGDA/PEGA). In all cases, only a single broad sub-glass relaxation is observed, designated as the  $\beta$  relaxation. The corre-

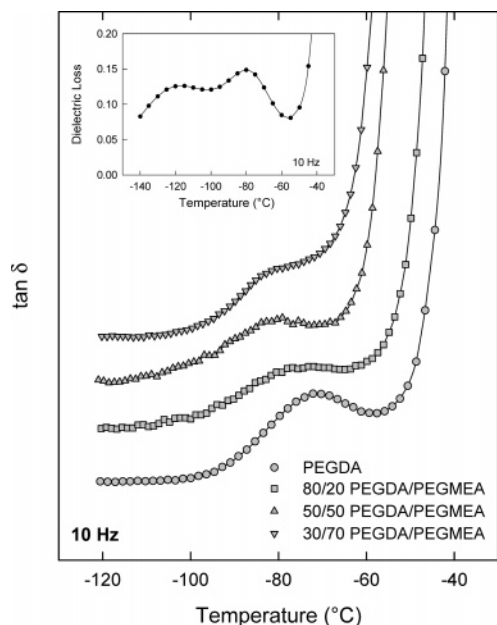


**Figure 5.**  $\tan \delta$  vs temperature for PEGDA/PEGMEA networks in the sub-glass transition range. Curves are offset vertically for clarity. Frequency of 10 Hz; heating rate of 1 °C/min. Inset: dielectric loss ( $\epsilon''$ ) vs temperature for 100% PEGDA network (10 Hz).<sup>25</sup>

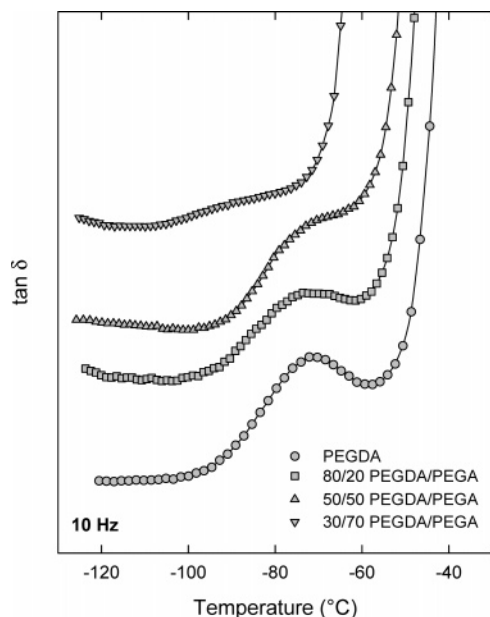


**Figure 6.**  $\tan \delta$  vs temperature for PEGDA/PEGA networks in the sub-glass transition range. Curves are offset vertically for clarity. Frequency of 10 Hz; heating rate of 1 °C/min.

sponding peak temperatures,  $T_\beta$ , are reported in Table 2. Sub-glass transitions in polymers typically reflect highly localized, noncooperative relaxation processes such as side-group rotations or limited in-chain motions.<sup>23</sup> For crystalline PEO, mechanical and dielectric investigations indicate two relaxation processes that originate in the amorphous regions of the polymer: a cooperative process corresponding to the glass transition and a noncooperative sub-glass process corresponding to local twisting modes along the PEO segments.<sup>23,24</sup> The relaxations observed for the wholly amorphous PEGDA networks would presumably have a similar origin, with the mechanical  $\beta$  transition reflecting limited motions occurring along the flexible ethylene oxide linkages.

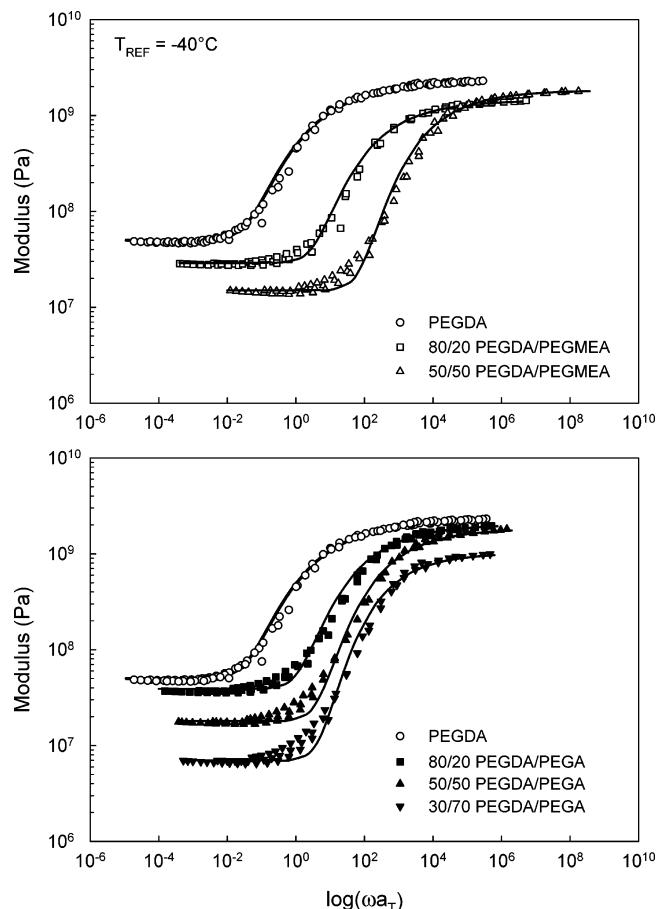


**Figure 7.** Time-temperature master curves for PEGDA copolymer networks;  $T_{\text{REF}} = -40$  °C. Solid curves are KWW best fits.

Interestingly, however, dielectric studies on cross-linked PEGDA and the copolymer networks consistently show two sub-glass transitions across the same temperature range (see inset, Figure 5).<sup>25</sup> Recently, Runt has reported dielectric results for crystalline PEO wherein two sub-glass relaxations were also observed, attributed to local mode motions occurring along amorphous PEO segments well-removed from the crystal surface and within more constrained segments located closer to the crystal amorphous interface, respectively.<sup>26</sup> For the cross-linked networks studied here, isolated motions well-removed from the cross-link junctions would have only a very weak influence on the bulk mechanical properties of the network, and they would be difficult to detect via dynamic mechanical measurements. As such, the single ( $\beta$ ) relaxation that is observed most likely reflects local motions that occur in relatively close proximity to the cross-link junctions, leading to a stronger overall mechanical response. This scenario is consistent with the observed negative shift in  $T_\beta$  with increasing acrylate content (re: PEGDA/PEGMEA series), as the resulting decrease in cross-link density and increased branch content would presumably lead to a less constrained local relaxation environment.

**Time-Temperature Superposition.** Time-temperature superposition was used to construct modulus-frequency master curves for the cross-linked networks at a common reference temperature of  $-40$  °C.<sup>17</sup> The results are shown in Figure 7, where the data are plotted as modulus vs  $\omega a_T$ , where  $\omega$  is the applied test frequency ( $\omega = 2\pi f$ , with  $f$  expressed in Hz) and  $a_T$  is

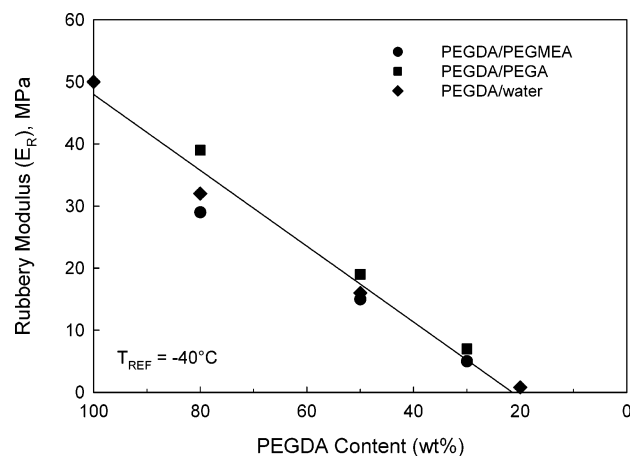


**Figure 8.** Rubbery modulus ( $E_R$ , MPa) vs PEGDA content for PEGDA/PEGMEA, PEGDA/PEGA, and PEGDA/water networks.  $E_R$  evaluated from time–temperature master curves at  $-40^\circ\text{C}$ .

the dimensionless shift factor. Data for the 30/70 PEGDA/PEGMEA network were not included in Figure 7, owing to the occurrence of cold crystallization in the dynamic mechanical temperature scan.

The glass–rubber relaxation can be satisfactorily described using the Kohlrausch–Williams–Watts (KWW) “stretched exponential” relaxation time distribution function:

$$\phi(t) = \exp[-(t/\tau_o)^\beta] \quad (1)$$

where  $\tau_o$  is the observed relaxation time and  $\beta$  is the distribution parameter.  $\beta$  ranges from 0 to 1, with values close to unity corresponding to a narrow, single relaxation time (i.e., Debye) response. Lower values of  $\beta$  typically reflect increased intermolecular coupling as well as inhomogeneous relaxation broadening owing to the presence of cross-links.<sup>7</sup> Series approximations reported by Williams et al. express modulus and loss for the KWW model in the frequency domain, and these equations were used as the basis for the curve fits reported here.<sup>18</sup>

Examination of the time–temperature master curves in Figure 7 clearly shows a systematic variation in relaxation time and rubbery modulus with increasing acrylate comonomer in the network. The rubbery plateau modulus ( $E_R$ ), as determined by the KWW fits at  $-40^\circ\text{C}$ , is plotted vs network composition in Figure 8. In addition to the data for the PEGDA/PEGMEA and PEGDA/PEGA series, results for networks based on PEGDA/water<sup>22</sup> (i.e., water diluent in the reaction mixture) are also included. According to classical rubber elasticity theory, the mechanical modulus measured in the rubbery plateau region should be proportional to the cross-link density.<sup>27–29</sup> In Figure 8, a single relationship is evident between rubbery modulus and PEGDA content for all three network systems. This implies that the effective cross-link density in the various networks depends solely on the amount of PEGDA cross-linker present in the reaction mixture, even though the structural details of the resulting networks may differ substantially.

In Figure 9, the KWW parameters ( $\tau_o$ ,  $\beta$ ) are plotted vs PEGDA content for the various networks. For both the PEGDA/PEGMEA and PEGDA/PEGA series,  $\tau_o$  decreases with decreasing PEGDA fraction at a fixed reference temperature. This behavior reflects the shift

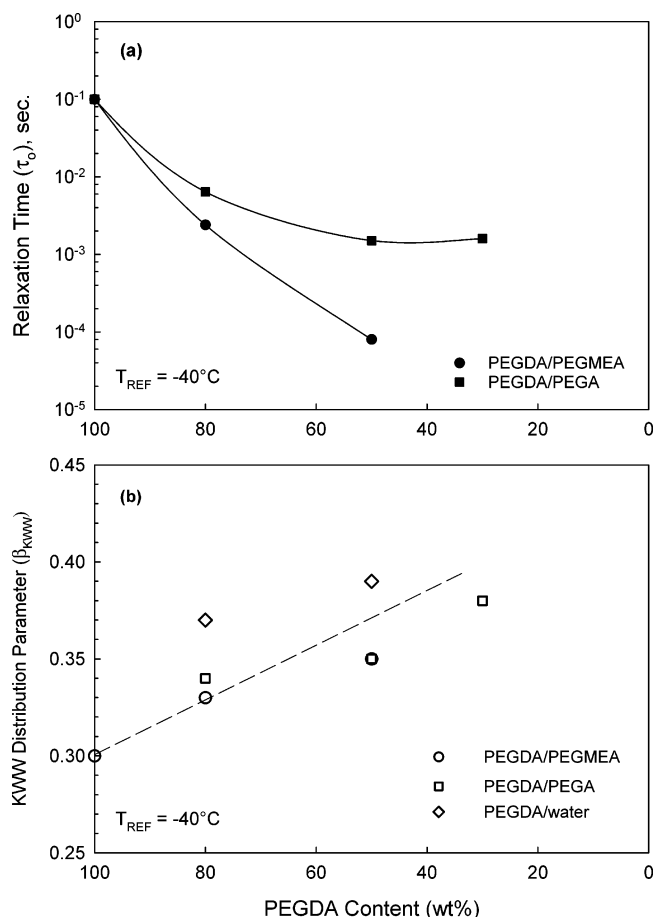


**Figure 9.** KWW parameters for the glass–rubber relaxation in PEGDA networks;  $T_{REF} = -40^\circ\text{C}$ . (a) Relaxation time ( $\tau_o$ , s) vs PEGDA content. (b) Distribution parameter ( $\beta_{KWW}$ ) vs PEGDA content.

in glass transition to lower temperatures (or higher frequencies) with increasing comonomer content. A decrease in PEGDA cross-linker also leads to a progressive increase in the KWW distribution parameter ( $\beta$ ), reflecting a narrowing of the glass–rubber relaxation with decreasing cross-link density; the trend is consistent across all three network systems examined. The observed narrowing of the glass–rubber relaxation with decreasing cross-link density suggests an overall reduction of the elastic constraints imposed by the cross-link junctions, leading to a more homogeneous segmental relaxation environment; this result is in agreement with KWW parameters reported for other networks of varying cross-link density.<sup>8–11,16</sup> For the networks examined here, comparable relaxation narrowing is observed regardless of the method used to reduce cross-link density, i.e., either through the addition of diluent to the reaction mixture or via copolymerization and the introduction of flexible pendant branches in the network.

**Cooperativity and Fragility.** The time–temperature character of the glass–rubber relaxation in the networks can be further examined by the construction of cooperativity or fragility plots, normalized Arrhenius plots wherein the shift factor ( $a_T = \tau/\tau_a$ ) is plotted as  $\log(a_T)$  vs  $T_a/T$  in the vicinity of the glass transition.<sup>7,19</sup> Figure 10 shows cooperativity plots for the PEGDA/PEGMEA and PEGDA/PEGA networks, based on the  $T_a$  values reported in Table 2. The solid curves correspond to WLF fits to the data. For both series of

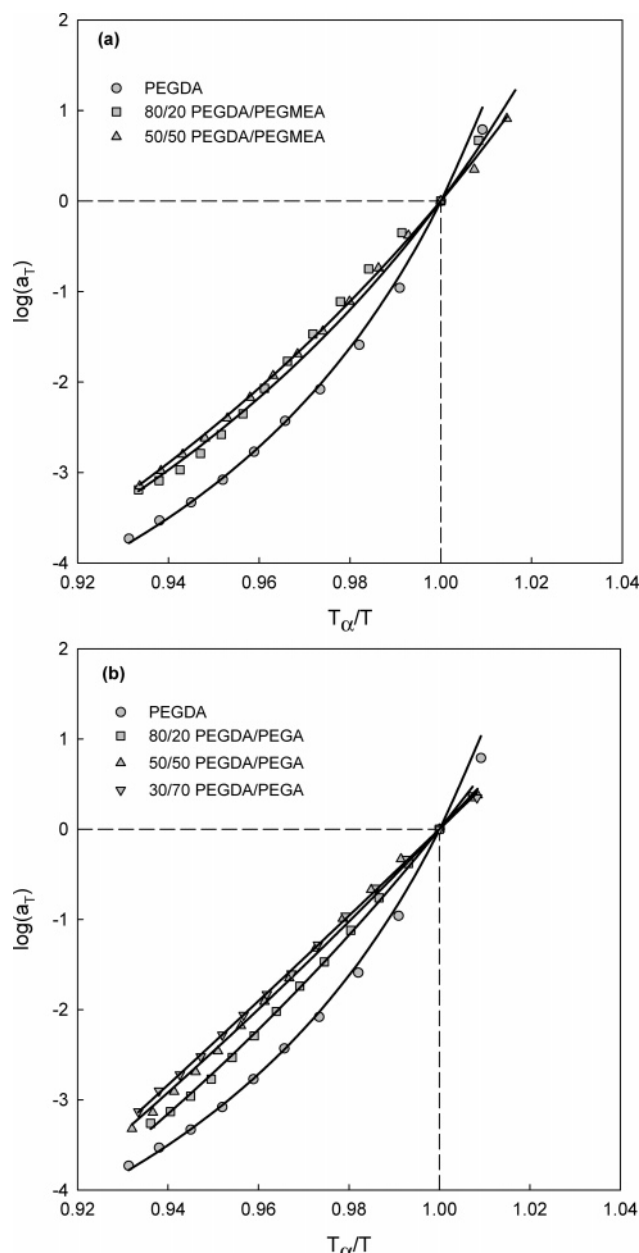


**Figure 10.** Cooperativity plots ( $\log(a_T)$  vs  $T_\alpha/T$ ) for PEGDA copolymer networks. Solid curves are WLF fits. (a) PEGDA/PEGMEA; (b) PEGDA/PEGA.

networks, the curves show a decrease in slope (i.e., decrease in time–temperature sensitivity) with decreasing cross-link density. This behavior suggests a net decrease in the intermolecular cooperativity inherent to the glass transition with a reduction in cross-link density and concomitant introduction of flexible PEG branches within the network. The trend is consistent with results reported for other homopolymer networks with varying cross-link density.<sup>7,8,16</sup>

The difference in time–temperature sensitivity and corresponding glass transition activation energy for the networks can be quantified in terms of the dynamic fragility of each material. Materials that display strong degradation of structure with temperature are designated as “fragile” liquids, and their relaxation typically reflects a high degree of intermolecular coupling. Polymers with smooth, flexible backbones tend to experience less intermolecular constraint and as a result display lower fragility.<sup>30</sup> This would likely be the case for

**Table 3.** Glass–Rubber Relaxation Characteristics for PEGDA and Copolymer Networks<sup>a</sup>

	$T_\alpha$ , °C	$E_A(T_\alpha)$	$m$
PEGDA	−35	354	78
PEGDA/PEGMEA			
80/20	−41	310	70
50/50	−47	262	60
PEGDA/PEGA			
80/20	−38	283	63
50/50	−41	231	52
30/70	−42	215	49

<sup>a</sup>  $T_\alpha$  is the dynamic mechanical peak temperature for glass transition (1 Hz),  $E_A(T_\alpha)$  the apparent activation energy (kJ/mol) evaluated at  $T_\alpha$ , and  $m$  the fragility index based on eq 2.

motions across the ethylene oxide segments present in the PEGDA networks.

The fragility index,  $m$ , corresponds to the slope of the cooperativity curve evaluated at  $T = T_{\text{REF}}$ :

$$m = \left. \frac{d \log(\tau)}{d(T_{\text{REF}}/T)} \right|_{T=T_{\text{REF}}} = \left. \frac{d \log(a_T)}{d(T_{\text{REF}}/T)} \right|_{T=T_{\text{REF}}} \quad (2)$$

where  $a_T = (\tau/\tau_{\text{REF}})$ . The value of  $m$  depends on the definition of  $T_{\text{REF}}$ : for the glass transition, the convention has been to assign  $T_{\text{REF}}$  such that the corresponding relaxation time  $\tau(T_{\text{REF}}) = 100$  s. Values of the fragility index determined on this basis range from  $m = 16$  (strong limit) to  $m \geq 200$  (fragile limit);<sup>31</sup> tabulations of dynamic fragility have been reported in the literature for a variety of polymers and small molecule glass formers.<sup>31–33</sup> The value of  $m$  can be related to the apparent activation energy ( $E_A$ ) evaluated at  $T_{\text{REF}}$ :

$$m = \frac{E_A(T_{\text{REF}})}{2.303RT_{\text{REF}}} \quad (3)$$

where  $R$  is the gas constant. For the fragility values reported here, we adopt a convention  $T_{\text{REF}} = T_\alpha$  (peak temperature at 1 Hz) which is more appropriate given the range of experimental frequencies used in our dynamic mechanical measurements (0.1–10 Hz). As such, the value of  $m$  should be considered a relative quantity, as it will vary depending upon the basis by which  $T_{\text{REF}}$  is assigned. Comparison of the fragility index with values reported in the literature is valid only if  $T_{\text{REF}}$  is assigned to the same relaxation time.

The activation energies,  $E_A(T_\alpha)$ , and fragility values for PEGDA and the copolymer networks are reported in Table 3. For both copolymer systems, a progressive decrease in the fragility value is evident with increasing acrylate content, indicating a lower degree of intermolecular cooperativity across the glass transition with decreasing cross-link density. A very similar result was obtained for the PEGDA/water networks, wherein cross-link density was varied by introducing water into the prepolymer reaction mixture.<sup>22</sup> For many materials, an inverse relation has been reported between the KWW distribution parameter ( $\beta$ ) and the fragility index ( $m$ ).<sup>31</sup> Increases in the distribution parameter, which are indicative of a narrowing of relaxation breadth, tend to correlate with a decrease in the fragility value. Such a correlation is observed for the PEGDA networks investigated here, as demonstrated in Figure 11.

The segmental relaxation characteristics of the PEGDA copolymer networks, and their relation to variations in cross-link density, are largely consistent with the



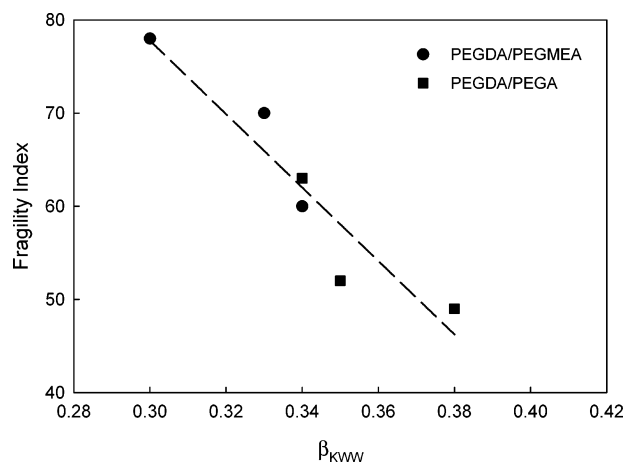


**Figure 11.** Fragility index ( $m$ ), as defined in eq 2, vs KWW distribution parameter ( $\beta_{\text{KWW}}$ ) for PEGDA copolymer networks.

behavior reported for other polymer networks with controlled cross-link density. The systematic decrease in cross-link density (with no net change in chemical composition) achieved by the copolymerization of flexible pendant groups into the network leads to a narrowing of the glass transition that reflects a more homogeneous relaxation environment, as the constraining influence of the acrylate junctions is reduced. This is accompanied by a decrease in fragility index, suggesting less intermolecular cooperativity inherent to the glass–rubber relaxation. These trends, which are common to many homopolymer network systems with varying cross-link density, would seem to indicate that the relaxation mechanism in the PEGDA networks is not substantially changed upon introduction of the pendant branches. That is, the segmental motions that occur along the ethylene oxide linkages of the branches ( $n = 7$  or 8 in length) are likely to be quite similar in character to those occurring across the cross-linked PEGDA bridges ( $n = 14$ ). As such, the underlying motional origin of the glass transition appears to remain more or less the same. However, the introduction of the pendant branches does lead to a decrease in the measured glass transition temperature for the copolymer networks, as the nonreactive chain ends introduce defects into the network structure. This effect is more pronounced for the PEGMEA comonomer ( $-\text{OCH}_3$  chain end) as compared to PEGA ( $-\text{OH}$  end group) and is accompanied by a systematic increase in fractional free volume for the PEGDA/PEGMEA series (refer to Table 2). Notably, for the PEGDA/PEGA series, a modest decrease in FFV is observed with increasing PEGA content.

**Gas Transport Properties.** Rubbery, amorphous polymer networks based on PEGDA have been identified as promising membrane materials for the selective removal of  $\text{CO}_2$  in mixtures with light gases such as  $\text{CH}_4$ ,  $\text{N}_2$ , and  $\text{H}_2$ .<sup>3</sup> One goal of the current work is to understand the relationships between structure and composition, cross-link density, and gas transport properties in these copolymer networks. Recent companion studies on cross-linked PEGDA and PEGDA copolymers detail the gas permeability and selectivity of these networks as a function of PEGDA content, cross-link density, and resulting fractional free volume.<sup>20,21</sup> Pure gas permeability measurements on the PEGDA/water series of networks have revealed that permeability is nearly independent of effective cross-link density when the fractional free volume (and corresponding glass transition temperature) of the network remains con-

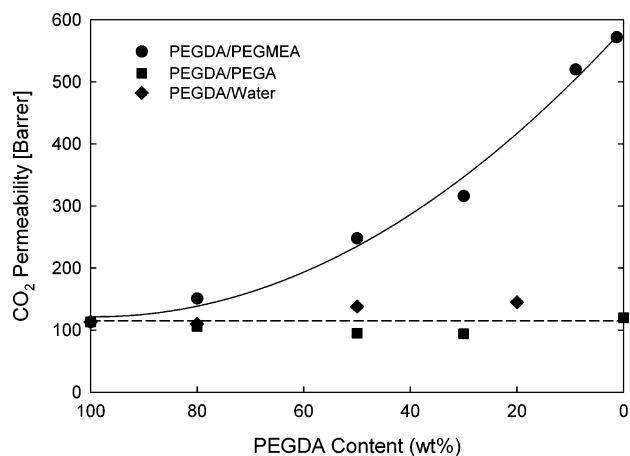


**Figure 12.**  $\text{CO}_2$  permeability (barrer) determined at 35 °C and infinite dilution for PEGDA networks.<sup>20,21</sup> 1 barrer =  $10^{-10} \text{ cm}^3 \text{ (STP) cm}/(\text{cm}^2 \text{ s cmHg})$ .

stant;<sup>20,22</sup> this result is shown in Figure 12, which contains representative permeability data for  $\text{CO}_2$  as a function of PEGDA content in the initial polymerization reaction mixture. A similar result is obtained in the PEGDA/PEGA networks, for which a modest decrease in  $\text{CO}_2$  permeability is observed with increasing PEGA content. The slight decrease in permeability that is observed for the PEGDA/PEGA series is consistent with a small decrease in estimated fractional free volume for these materials as reported in Table 2. The behavior for the PEGDA/PEGA networks is in sharp contrast to the results for the PEGDA/PEGMEA series, where a dramatic increase in  $\text{CO}_2$  permeability is observed with increasing PEGMEA branch content in the rubbery network (see Figure 12); this increase is driven primarily by an increase in the diffusivity of  $\text{CO}_2$  in the polymer, as ethylene oxide content (and corresponding  $\text{CO}_2$  solubility) remains virtually unchanged over the range of copolymer compositions.<sup>21</sup> The increase in  $\text{CO}_2$  pure gas permeability correlates directly with the measured increase in fractional free volume for this polymer series. In addition, the PEGDA networks display favorable pure gas selectivity for reverse-selective separations (e.g., preferential permeation of  $\text{CO}_2$  over  $\text{H}_2$ ). For 100% cross-linked PEGDA, pure gas  $\text{CO}_2/\text{H}_2$  selectivity ( $\alpha = P_{\text{CO}_2}/P_{\text{H}_2}$ ) has a value of  $\sim 8$  for measurements conducted at 35 °C; this value remains nearly constant across both the PEGDA/water and PEGDA/PEGA series of networks. For the PEGDA/PEGMEA copolymer series, a progressive increase in selectivity is observed with increasing PEGMEA content: a  $\text{CO}_2/\text{H}_2$  selectivity value of 13 is measured for minimally cross-linked networks containing 99 wt % PEGMEA.

The contrasting gas transport performance observed for the PEGDA/PEGMEA and PEGDA/PEGA copolymer series demonstrates the sensitivity of these materials to minor changes in network structure or composition. In the case of the copolymer networks, the only obvious difference is the nature of the end group on the pendant branches:  $-\text{OCH}_3$  vs  $-\text{OH}$ . This distinction leads to much greater variations in glass transition temperature and permeability across the PEGDA/PEGMEA series as compared to the PEGDA/PEGA specimens, variations that correlate primarily with the fractional free volume contained in the network. One possible explanation for the observed difference in these copolymer series is the potential for the  $-\text{OH}$  chain ends in the PEGDA/PEGA



polymers to form hydrogen bonds within the network structure, leading to local interactions that could potentially offset the changes in  $T_g$  and free volume typically encountered with the insertion of branchlike defects. The sensitivity of these membranes to relatively small variations in structure highlights the importance of developing fundamental understanding regarding how such changes influence membrane performance properties and how intelligent design and control of membrane structure can be exploited to optimize separation performance for specific applications.

## Conclusions

The relaxation characteristics of two series of rubbery networks based on PEGDA copolymerized with either PEGMEA or PEGA were investigated by dynamic mechanical analysis. The introduction of monofunctional acrylate in the prepolymer reaction mixture was used to control cross-link density in the resulting polymers and led to the insertion of flexible oligomeric branches within the networks; the molecular weights of the PEGMEA and PEGA co-components were selected so as to maintain a constant ethylene oxide content within the final networks. For both series, the introduction of the acrylate comonomer led to a decrease in the measured glass transition temperature as well as a systematic reduction in cross-link density as reflected in the rubbery modulus of the network. KWW curve fits to time-temperature modulus master curves indicated a narrowing of the glass-rubber relaxation with reduced cross-link density that correlated with a decrease in fragility, suggesting a more homogeneous, less cooperative relaxation environment in the copolymer networks. The influence of the copolymer branches was more pronounced in the PEGDA/PEGMEA series, which displayed a much larger variation in glass transition temperature with changing PEGDA content. A contrast was also evident in the gas transport properties of the two network series, with the PEGDA/PEGMEA membranes displaying a strong variation in permeability and selectivity over the range of copolymer compositions examined. Both the observed glass transition and transport behavior correlated with measured variations in fractional free volume for these networks.

**Acknowledgment.** This research was supported in part by a grant from the Kentucky Science and Engineering Foundation as per Grant Agreement KSEF-148-502-05-130 with the Kentucky Science and Technology Corp. We are also pleased to acknowledge support provided through a Kentucky Opportunity Fellowship administered by the University of Kentucky Graduate School (S.K.). Activities at the University of Texas at Austin were supported in part by the Chemical Sciences, Geosciences and Biosciences Division, Office of Basic Energy Sciences, Office of Science, U.S. Department of Energy (Grant DE-FG03-02ER15362). This research work was also partially supported with funding from the United States Department of Energy National Energy Technology Laboratory under a subcontract from Research Triangle Institute through their Prime

Contract No. DE-AC26-99FT40675. This work was prepared with the partial support of U.S. Department of Energy, under Award DE-FG26-01NT41280. Any opinions, findings, conclusions, or recommendations expressed herein are those of the authors and do not necessarily reflect the views of the DOE.

## References and Notes

- (1) Baker, R. W. *Membrane Technology and Applications*, 2nd ed.; John Wiley and Sons: New York, 2004.
- (2) Koros, W. J. *J. Polym. Sci., Part B: Polym. Phys.* **1985**, *23*, 1611–1628.
- (3) Lin, H.; Freeman, B. D. *J. Mol. Struct.* **2005**, *739*, 57–74.
- (4) Lin, H.; Freeman, B. D. *J. Membr. Sci.* **2004**, *239*, 105–117.
- (5) Priola, A.; Gozzelino, G.; Ferrero, F.; Malucelli, G. *Polymer* **1993**, *34*, 3653–3657.
- (6) Graham, N. B. In *Hydrogels in Medicine and Pharmacy*; Peppas, N. A., Ed.; CRC Press: Boca Raton, FL, 1987; Vol. 2, pp 95–113.
- (7) Roland, C. M. *Macromolecules* **1994**, *27*, 4242–4247.
- (8) Schroeder, M. J.; Roland, C. M. *Macromolecules* **2002**, *35*, 2676–2681.
- (9) Kannurpatti, A. R.; Anderson, K. J.; Anseth, J. W.; Bowman, C. N. *J. Polym. Sci., Part B: Polym. Phys.* **1997**, *35*, 2297–2307.
- (10) Kannurpatti, A. R.; Anseth, J. W.; Bowman, C. N. *Polymer* **1998**, *39*, 2507–2513.
- (11) Kannurpatti, A. R.; Bowman, C. N. *Macromolecules* **1998**, *31*, 3311–3316.
- (12) Fitz, B. D.; Mijovic, J. *Macromolecules* **1999**, *32*, 3518–3527.
- (13) Glatz-Reichenbach, J. K. W.; Sorriero, L. J.; Fitzgerald, J. J. *Macromolecules* **1994**, *27*, 1338–1343.
- (14) Yu Kramarenko, V.; Ezquerro, T. A.; Sics, I.; Balta-Calleja, F. J.; Privalko, V. P. *J. Chem. Phys.* **2000**, *113*, 447–452.
- (15) Litvinov, V. M.; Dias, A. A. *Macromolecules* **2001**, *34*, 4051–4060.
- (16) Alves, N. M.; Gomez Ribelles, J. L.; Gomez Tejedor, J. A.; Mano, J. F. *Macromolecules* **2004**, *37*, 3735–3744.
- (17) Ferry, J. D. *Viscoelastic Properties of Polymers*, 3rd ed.; John Wiley and Sons: New York, 1980.
- (18) Williams, G.; Watts, D. C.; Dev, S. B.; North, A. M. *Trans. Faraday Soc.* **1971**, *67*, 1323–1335.
- (19) Angell, C. A. *J. Non-Cryst. Solids* **1991**, *131–133*, 13–31.
- (20) Lin, H.; Kai, T.; Freeman, B. D.; Kalakkunnath, S.; Kalika, D. S. *Macromolecules* **2005**, *38*, 8381–8393.
- (21) Lin, H.; Van Wagner, E.; Swinnea, J. S.; Freeman, B. D.; Pas, S. J.; Hill, A. J.; Kalakkunnath, S.; Kalika, D. S. *J. Membr. Sci.*, in press.
- (22) Kalakkunnath, S.; Kalika, D. S.; Lin, H.; Freeman, B. D., submitted to *J. Polym. Sci., Part B: Polym. Phys.*
- (23) McCrum, N. G.; Read, B. E.; Williams, G. *Anelastic and Dielectric Effects in Polymeric Solids*; John Wiley and Sons: London, 1967.
- (24) Ishida, Y.; Matsuo, M.; Takayanagi, M. *J. Polym. Sci., Polym. Lett.* **1965**, *3*, 321–324.
- (25) Kalakkunnath, S.; Kalika, D. S.; Lin, H.; Freeman, B. D., manuscript in preparation.
- (26) Jin, X.; Zhang, S.; Runt, J. *Polymer* **2002**, *43*, 6247–6254.
- (27) Treloar, L. R. G. *The Physics of Rubber Elasticity*, 3rd ed.; Oxford University Press: New York, 1975.
- (28) Mark, J. E. *Rubber Chem. Technol.* **1982**, *55*, 762–768.
- (29) Hill, L. W. *Prog. Org. Coat.* **1997**, *31*, 235–243.
- (30) Ngai, K. L.; Roland, C. M. *Macromolecules* **1993**, *26*, 6824–6830.
- (31) Bohmer, R.; Ngai, K. L.; Angell, C. A.; Plazek, D. J. *J. Chem. Phys.* **1993**, *99*, 4201–4209.
- (32) Roland, C. M.; Santangelo, P. G.; Ngai, K. L. *J. Chem. Phys.* **1999**, *111*, 5593–5598.
- (33) Huang, D.; McKenna, G. B. *J. Chem. Phys.* **2001**, *114*, 5621–5630.

MA051741T